Ice sheet dynamics

①

References: R. LeB. Hooke, Principles of Glacier Mechanics, Cambridge Univ. Press, 2005
W.S.B. Paterson, The Physics of Glaciers, 3rd ed., 1994.
Oerlemans, J. and C.J. van der Veen, Ice Sheets and Climate, Reidel, Dordrecht, 1984

ICE SHEETS

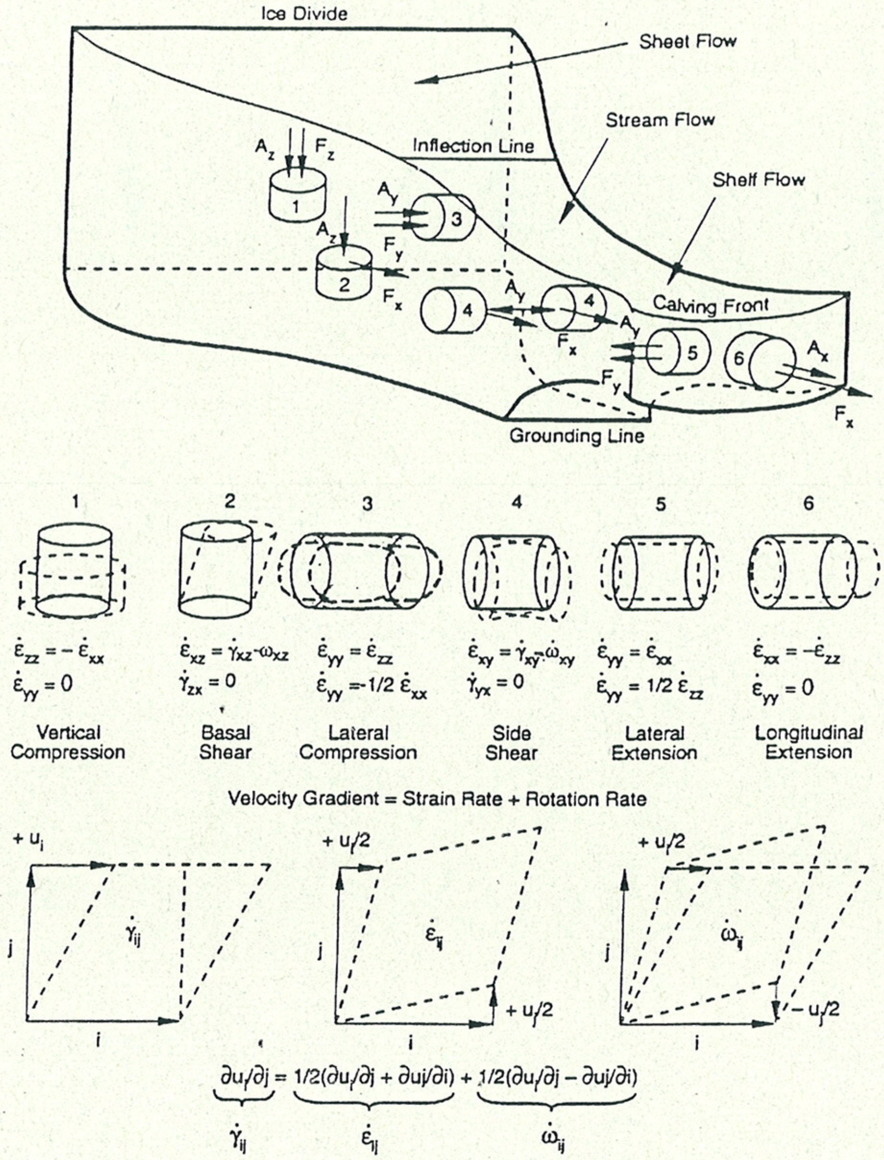

Figure 4.2: The major deviator stresses from the ice divide to the calving front for a flowband along which sheet flow becomes stream flow and stream flow becomes shelf flow. The cylinders of ice are greatly enlarged and are deformed by deviator stresses σ_{ij}'. In plan view, axis x is along the flowband, axis y is transverse to the flowband, and axis z is vertical. *Cylinder 1*: For vertical compression beneath a linear ice divide, $\sigma_{zz}' = F_z / A_z$, $\dot{\varepsilon}_{zz} = -\dot{\varepsilon}_{xx}$, and $\dot{\varepsilon}_{yy} = 0$. *Cylinder 2*: For simple shear at the bed, $\sigma_{xz} = F_x / A_z$, $\dot{\varepsilon}_{xz} = \dot{\gamma}_{xz} - \dot{\omega}_{xz}$, and $\dot{\gamma}_{zx} = 0$. *Cylinder 3*: For transverse compression from converging flow, $\sigma_{yy}' = F_y / A_y$, $\dot{\varepsilon}_{yy} = \dot{\varepsilon}_{zz}$, and $\dot{\varepsilon}_{yy} = -1/2\ \dot{\varepsilon}_{xx}$. *Cylinder 4*: For simple shear at the sides, $\sigma_{xy}' = F_x / A_y$, $\dot{\varepsilon}_{xy} = \dot{\gamma}_{xy} - \dot{\omega}_{xy}$, and $\dot{\gamma}_{yx} = 0$. *Cylinder 5*: For transverse extension from diverging flow, $\sigma_{yy}' = F_y / A_y$, $\dot{\varepsilon}_{yy} = \dot{\varepsilon}_{xx}$, and $\dot{\varepsilon}_{yy} = -\ 1/2\ \dot{\varepsilon}_{zz}$. *Cylinder 6*: For longitudinal extension along a linear calving front, $\sigma_{xx}' = F_x / A_x$, $\dot{\varepsilon}_{xx} = -\dot{\varepsilon}_{zz}$, and $\dot{\varepsilon}_{yy} = 0$. By definition, for velocities u_i and u_j in directions i and j, $\dot{\gamma}_{ij} = \partial u_i / \partial j$ is the velocity gradient, $\dot{\varepsilon}_{ij} = 1/2\ (\partial u_i / \partial j + \partial u_j / \partial i)$ is the strain rate, and $\dot{\omega}_{ij} = 1/2\ (\partial u_i / \partial j + \partial u_j / \partial i)$ is the rotation rate, so $\dot{\gamma}_{ij} = \dot{\varepsilon}_{ij} + \dot{\omega}_{ij}$.

Hughes, 1998

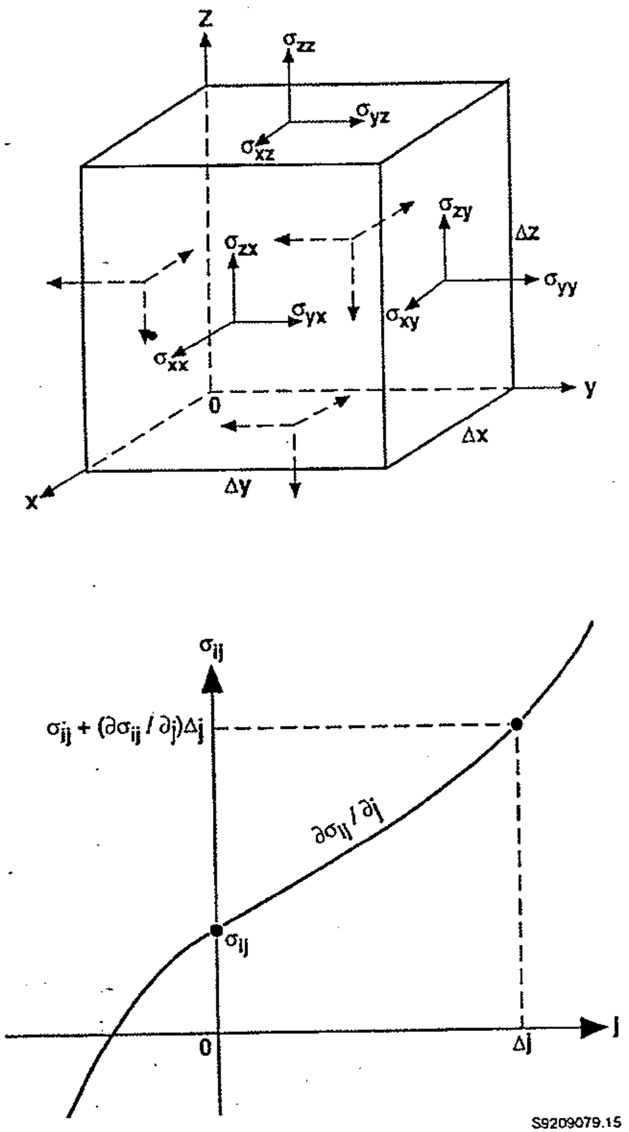

Figure 4.5: The force of balance used for deriving the equilibrium equations. Forces from kinematic stresses σ_{ij} acting normal and parallel to faces of a body having lengths Δx, Δy, Δz along rectilinear axes x, y, z are balanced by gravitational body forces and forces from kinematic stresses $\sigma_{ij} + (\partial\sigma_{ij}/\partial j)\ \Delta j$ acting normal and parallel to the opposite faces, where stress gradients $\partial\sigma_{ij}\ /\partial j$ are constant within the body and i, j = [illegible] y, z in the usual tensor notation. Stresses σ_{ij} on a given fa[illegible] (top) are stress differences $[\sigma_{ij} + (\partial\sigma_{ij}\ /\partial j)\ \Delta j] - \sigma_{ij}$ across opposite

Benn & Evans (1998)

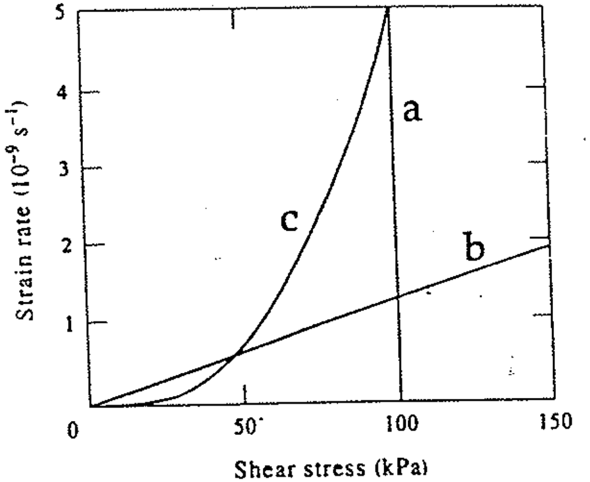

Fig. 4.8 Stress–strain relationships for different types of material. (a) Perfectly plastic material, which remains rigid until the shear stress reaches the yield stress (100 kPa in this case), when it deforms instantaneously; (b) Newtonian viscous material, for which the strain rate is linearly proportional to shear stress; (c) non-linearly viscous material, such as ice. (Modified from Paterson, 1994)

Paterson (1994)

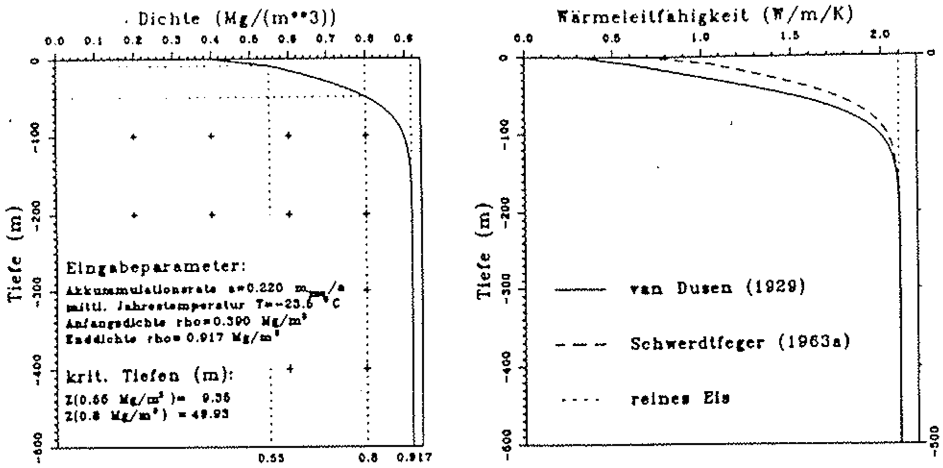

Abbildung 2.1: Dichte-Tiefen-Funktion im Bereich der Filchner-Station nach dem Modell von Herron & Langway (1980) (links) und Wärmeleitfähigkeit nach Van Dusen (1929) und Schwerdtfeger (1963a) (rechts)

Grosfeld, 1993

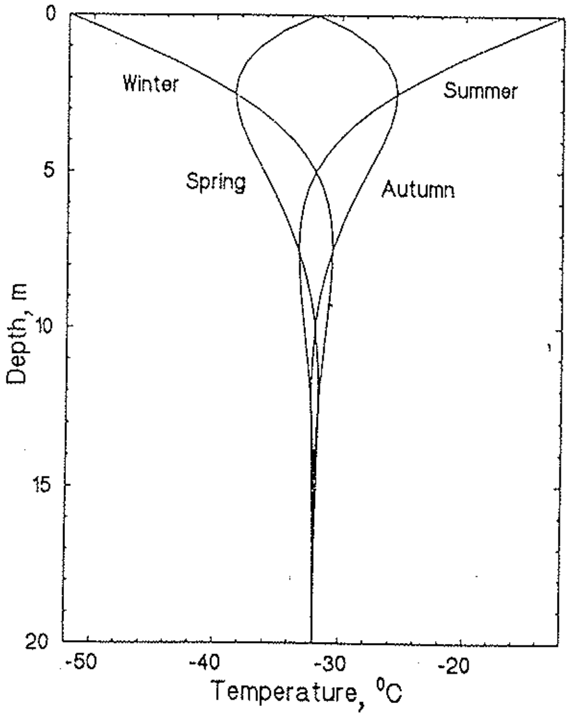

FIG. 10.1. Calculated seasonal variations in firn temperature in central Greenland.

Paterson, 1994

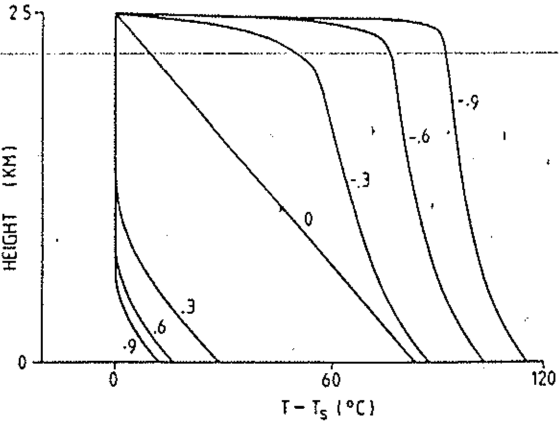

Figure 5.1. Temperature profiles (steady state) for an ice sheet which is 2500 m thick. Labels give the accumulation rate at the surface in m ice depth / yr.

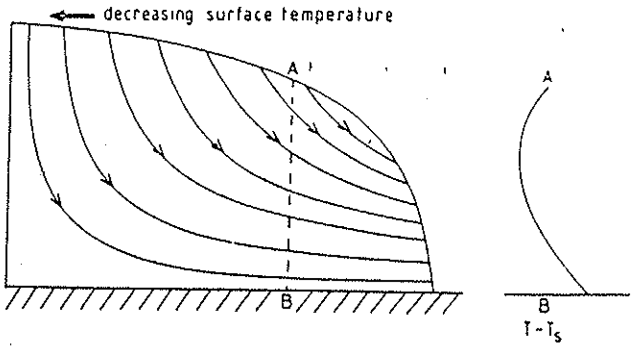

Figure 5.2. Reversal of temperature gradient in the upper layers when advection becomes important.

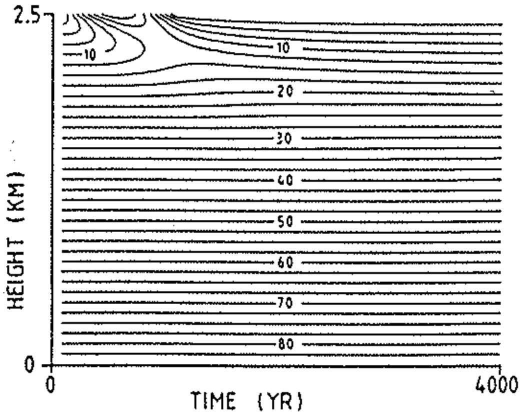

Figure 5.3. Downward penetration of a perturbation in surface temperature by conduction only. Temperature is given with respect to undisturbed surface temperature (K).

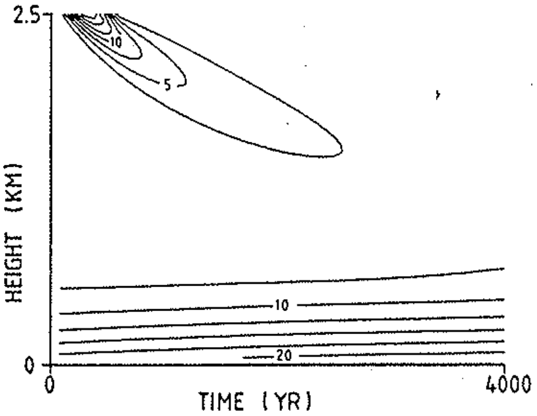

Figure 5.4. As in Figure 5.3, now taking into account downward advection.

Lit.: Oerlemans & van der Veen, 198

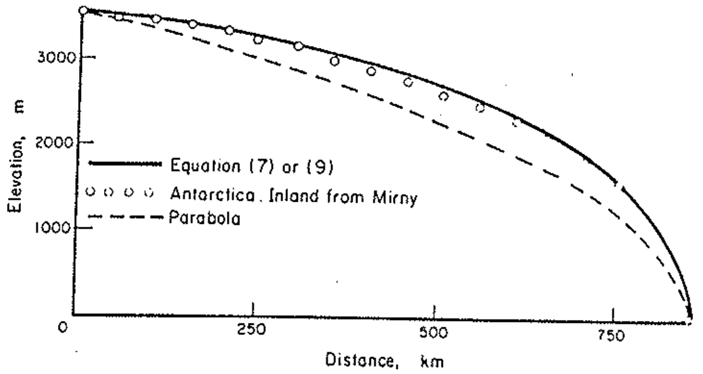

Fig. 9.2. Profile of Antarctic Ice Sheet inland from Mirny, compared with theoretical profiles. Data from Vialov (1958).

Paterson, 1994